

Magnetically insulated high-gradient accelerating structures for muon accelerators

This article has been downloaded from IOPscience. Please scroll down to see the full text article.

2010 J. Phys. G: Nucl. Part. Phys. 37 105011

(<http://iopscience.iop.org/0954-3899/37/10/105011>)

View [the table of contents for this issue](#), or go to the [journal homepage](#) for more

Download details:

IP Address: 76.89.129.189

The article was downloaded on 24/08/2010 at 08:09

Please note that [terms and conditions apply](#).

Magnetically insulated high-gradient accelerating structures for muon accelerators

Diktys Stratakis¹, Juan C Gallardo and Robert B Palmer

Department of Physics, Brookhaven National Laboratory, Upton NY 11973, USA

Received 20 April 2010

Published 24 August 2010

Online at stacks.iop.org/JPhysG/37/105011

Abstract

Reduction of the available accelerating gradient in cavities exposed to external magnetic fields is a longstanding problem which limits the performance of many systems, especially muon accelerators. We propose a novel idea for improving the cavity's gradient by suppressing breakdown events caused by field emissions on its surfaces. The concept involves designing an rf cavity wherein its walls are parallel to the contour lines of the external magnetic fields, thereby preventing field-emitted electrons from leaving the surface, and subsequently picking up energy from the rf electric field. We present a conceptual design of a muon accelerator cooling lattice with magnetically insulated cavities and detail its expected performance. Our results suggest that the magnetically insulated cooling channel we describe, although demanding in rf power, can produce enough initial beam cooling to be a feasible option for a muon collider or a neutrino factory.

(Some figures in this article are in colour only in the electronic version)

1. Introduction

There is a growing interest in machines that transport and accelerate muons rather than the traditional electrons or protons [1]. Unlike electrons, muons can be accelerated in circular machines, thus permitting the re-use of rf- and magnetic elements, so conferring a smaller foot print and, hence, lowering engineering costs [2]. Since the phase space of the muon beam that comes from pion decays exceeds the acceptance of downstream accelerator systems, a cooling channel is required to reduce the transverse and longitudinal emittance [3]. Because the lifetime of a muon is short ($\tau = 2.2 \mu\text{s}$), the only technique fast enough is ionization cooling [4, 5]. In this process, the magnitude of the transverse- and longitudinal momenta is reduced by energy loss in the ionization media, followed by subsequent restoration of the longitudinal momentum component with rf power.

¹ Present address: Department of Physics & Astronomy, University of California, Los Angeles CA 90095, USA.

Muon collider lattices that have been designed and simulated provide the required cooling, but they required the rf cavity to operate in strong axial magnetic fields that focuses the muons [6, 7]. Typical rf frequencies on those lattices range from 201 to 805 MHz, with gradients from 16 to 25 MV m⁻¹, and the magnetic fields at the cavities ranges from 2.5 to 5 T. Any decrease in the rf gradient from its specified values proved deleterious, since it was accompanied by a drop in the transmission of muons due their fast decay [7].

Three experiments at the MuCool Test Area (MTA) at Fermi National Laboratory (FNAL) explored the efficiency of pillbox rf cavities within magnetic fields: the first had a multi-cell 805 MHz cavity [8]; the second had a single 201 MHz one [9] and the third a single 805 MHz cavity [10]. All three trials showed that rf cavities did not operate well in external magnetic fields. In particular, the cavity windows in the first were punctured, and the second and third experiments revealed significant reductions in the maximum achievable rf gradients when the field was turned on; inspection of the cavities' surfaces noted severe damage also [11]. According to a recent theory [12], this gradient drop in the presence of an external magnetic field occurs after electrons from a field-emission site [13] damage a surface with high electric fields. Such surface damage would result by fatigue [14, 15] from cyclical strains induced by local heating from the electrons. This theory agrees reasonably well with numerical simulations [16] and experimental data [10].

As mentioned, cooling channels typically rely on rf cavities operating in high magnetic fields, so it is crucial to demonstrate that the technology is feasible and reliable. Since the gradient of conventional pillbox cavities is limited by rf breakdown, likely due field emission, the intent of our present work is to design a 'magnetically insulated' rf cavity, and study its application to muon ionization cooling lattices. Magnetic insulation is a concept well known in applications with pulsed voltages [17–19]. The underlying principle is that a magnetic field can prevent an electrical breakdown by diverting the electron-flow generated and accelerated by a high-intensity electric field.

So far, magnetic insulation for an rf cavity has never been used, making this a new and novel concept. In this paper, we demonstrate that by designing a magnetically insulated cavity such that its walls are parallel to chosen magnetic-field contour lines, we can suppress damage from field emission. We then detail its application to cooling channels for a muon accelerator, and present a conceptual representation of a muon-transport lattice with magnetically insulated cavities. We demonstrate ionization cooling with such a lattice, and compare its performance against a conventional lattice with pillbox cavities. Our findings indicate that a lattice with magnetically insulated cavities is a satisfactory alternative option for the front end of a neutrino factory or a muon collider.

The outline of this paper is as follows: In section 2, we overview the observed problems in operating rf in magnetic fields. In section 3, we illustrate the simulation of field emission with and without external magnetic fields within a conventional 'pillbox' and within a magnetically insulated cavity. In section 4, we examine the performance of a muon cooling channel with magnetically insulated rf cavities. Finally, our conclusions are given in section 5.

2. Problems with rf cavities in magnetic fields

Designs of muon ionization cooling channels for a neutrino factory or muon collider require very high-gradient rf accelerating structures. Depending on which cooling stage is considered, rf cavities are needed in the range of 201 to 805 MHz, with peak accelerating gradients, respectively, of 16 MV to 25 MV m⁻¹. Figure 1 depicts a conventional muon-accelerator cavity with an 805 MHz frequency. The configuration of the cavity adopts cylindrically symmetrical pillbox geometry, with a conventional beam irises covered with metallic Be

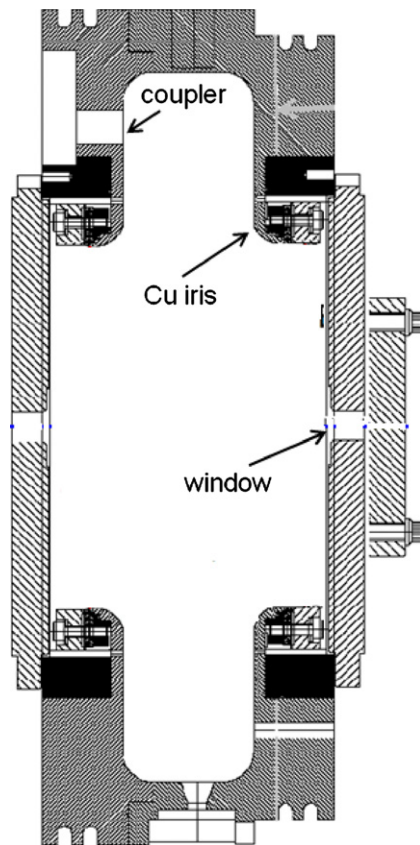


Figure 1. Layout of a conventional muon cooling 805 MHz pillbox cavity.

Table 1. Characteristics of the rf system.

	Pillbox	Magnetically insulated
rf frequency (MHz)	805	805
Axial cavity length (cm)	8.1	16.0
Cavity radius (cm)	15.0	12.7
$Q/10\,000$	2.01	1.77
Shunt impedance ($M\Omega\ m^{-1}$)	42.0	21.3
B_{\max}/E_{\max} ($mT\ MV^{-1}\ m^{-1}$)	2.27	2.08
E_{\max}/E_0	1.06	2.40
Power for $E_0 = 25\ MV\ m^{-1}$ (MW)	1.2	4.7

windows. Table 1 lists the parameters of this cavity; a more detailed description is given elsewhere [20].

The multi-cell-cavity [8] and pillbox-cavity [9, 10] experiments involved a cavity similar to that shown in figure 1, and all revealed major problems. In particular, in the multi-cell cavity, even though the acceleration gradients seemed to be little affected by the field, the dark

current was enhanced greatly when the magnetic field was on. After some time and still with the field on, the cavity's titanium vacuum window was damaged, and its vacuum lost. In a later test of a single 805 MHz 'pillbox' cavity (see figure 1) with beryllium (Be) or copper (Cu) windows, the cavity was sited at the center of the magnet and the field was uniform in its interior. As the strength of the magnetic field was raised from 0 to 4 T, measurements recorded a reduction in the maximum gradient by 60%. Also, there was considerable pitting on surfaces of the copper iris. More recently, a test of a 201 MHz cavity [9] without a field achieved 21 MV m^{-1} , but in the 0.6 T fringe field of a 4.5 T magnet, 10 MV m^{-1} was reached; when tested again without a field, the cavity could not again attain more than 18 MV m^{-1} . So, in all cases, the operation of the rf in magnetic fields, equal to or even less than those specified, caused damage, and mostly showed a serious decline in the achievable gradient.

3. Field emission with and without external magnetic fields

3.1. Pillbox cavity

A new published theory [12, 16] assumes that the breakdown in magnetic fields occurs after electrons from field emission damage a surface with high electric fields. To examine this phenomenon further, we numerically assessed field emissions within the pillbox cavity. For the simulation, we used CAVEL [21], a code that tracks particles from arbitrary positions on the walls of a cavity until their final position on some other surface. The program uses SUPERFISH [22] to determine the rf electric fields and the magnetic fields, and uses a map of external magnetic fields calculated for arbitrary coil dimensions and currents. Figure 2 shows the tracks of electrons departing from the highest surface rf electric field point. Our simulation assumed a pillbox 805 MHz cavity identical to that shown in figure 1, and a 20 MV m^{-1} maximum axial gradient. Figure 2(a) shows the trajectories without external magnetic fields; figure 2(b) shows tracking with a uniform 0.5 T one. The multiple trajectories correspond to the different initial phases, given in degrees, with respect to that with a maximum initial rf field.

Without an external magnetic field it can be shown that, none of the trajectories from the high-field location return to their common origin. Tracks emitted at zero field hit the opposing iris at a high-field location, but are not focused there; instead, they spread out over a significant distance. However, as the axial magnetic field is raised the tracks either are focused to the high-gradient location on the following iris, or are returned to their original emission point.

Figure 3 shows the energies of the electrons on impact for the 0.5 T field case, and indicates which phases are returned (open circles) and which arrive on the next iris (solid squares). The blue solid line depicts the corresponding relative current $I_\phi / I_{\phi=0^\circ}$, assuming that field emission follows the Fowler–Nordheim relation [23], $I_\phi = 1.54 \times 10^{-6} \frac{A_e \beta_e^2 E_\phi^2}{w} 10^{4.52w^{-0.5}} \left(e^{-\frac{6.53 \times 10^9 w^{1.5}}{\beta_e E_\phi}} \right)$ and thus scales as a power law with the rf phase ϕ . Note that in the above expression, E_ϕ is the rf electric field (in V m^{-1}) at a given ϕ , w is the metal's work function in eV, β_e is the field enhancement and A_e is the emitting area (in m^2). We assume that $E_\phi = E_0 \cos \phi$, where E_0 is the gradient at $\phi = 0^\circ$. Since field-emitted electrons within the range of $\pm 25^\circ$ are focused to a local area on the opposite iris, it seems unlikely that significant currents of electrons will return to their source. Note that the electron impact energies are approximately 1 MeV. Detailed tracking simulations in [16] suggested that when the magnetic field is of the order of a tesla, the delivered power density of those energetic electrons is sufficient to induce fatigue and damage into the cavity surface.

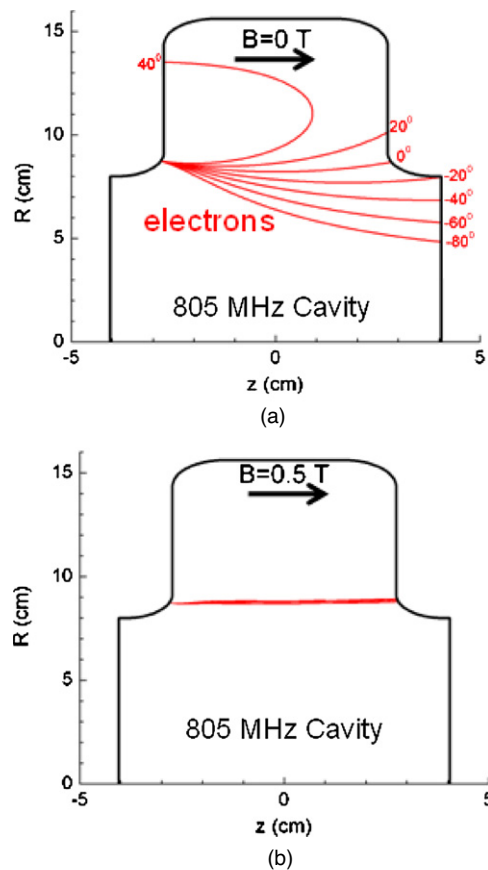


Figure 2. Trajectories of field-emitted electrons at different rf phases from the highest surface electric field location within the pillbox cavity shown in figure 1: (a) with no external magnetic field and, (b) with an axial and uniform 0.5 T magnetic field.

3.2. Magnetically insulated cavity

We could suppress the damage caused from field-emitted electrons by designing rf cavities such that all high gradient surfaces were parallel to the external magnetic field. Instead of focusing electrons, the field then would return them, with little energy, to near their points of origin. Figure 4(a) illustrates our proposed magnetically insulated cavity. The cavity has two open irises, and its shape is constrained by the geometry of the two inner elliptical coils which, as we will show in the next section, will serve as to focus the muon beam. Note that the cavity's walls follow the magnetic-field lines that those coils generate. Note further that the outer bucking coils serve to modify the field lines so as to improve the cavity's shape and performance. Table 1 lists the main design parameters of this cavity.

Like in the pillbox rf case we simulated field emissions within a magnetically insulated cavity via CAVEL; the results appear in figure 4(b). In the results shown herein the electrons are tracked from the location of the highest surface rf electric field (arrow in figure 4(a)). We interpret the data as follows: emitted electrons initially are accelerated by the electric field away from that surface. Then, as they attain significant momentum, the magnetic field

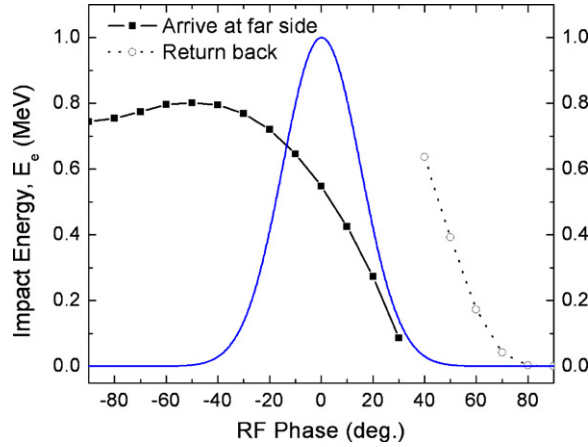


Figure 3. Energies of electrons on impact versus their phase of emission. Solid squares indicate electrons that arrive on the next iris (like in figure 2(b)). Open circles indicate electrons that returned to their emission site. The solid blue line shows the relative current at a given rf phase and is normalized to its maximum value at $\phi = 0^\circ$. The axial electric field is $E_0 = 20 \text{ MV m}^{-1}$.

deflects them and directs them back to the surface. Depending on their phase of emission, they may return to the surface after a single half-loop, or they may make several loops, but they always return to the surface. Figure 5 shows their corresponding impact energies versus phase. We choose three different accelerating gradients, which are within the typical operating range for a muon accelerator. Interestingly, in all the cases, the impact energy is lower by three orders of magnitude than that with the pillbox cavity (i.e. $E_e < 1 \text{ keV}$). Thus, as we will quantitatively demonstrate in the next paragraph, it is likely that much less damage may occur on the surface. One difficulty might arise due to multipacting, since now, the energies with which electrons return to surfaces are in the range of a few hundred eV where secondary emissions are maximal. However, a simulation conducted at SLAC revealed no problems from multipacting inside this insulated cavity [24].

We can calculate a lowest order estimate of the required energy to damage the cavity. When the electrons strike the cavity wall, the surface temperature rises by [12]

$$\Delta T = \frac{I\tau}{q\pi\sigma_r^2\rho c_s} S, \quad (1)$$

where c_s is the specific heat, I is the current, q is the electron charge, ρ the cavity's material density, σ_r is the radius of the spot the electrons create on impact, τ is the rf pulse length, taken as $20 \mu\text{s}$ at 805 MHz [10] and $S = dE_e/dx$ is the stopping power with the penetration depth x . For simplicity, we assumed that the damaged spot was round. Then, its radius scales as [16] $\sigma_r = c_2 I^j / B$, where B is the external magnetic field and c_2, j are fitting constants.² Inserting this expression into equation (1) we have

$$\Delta T = \frac{B^2\tau}{q\pi c_2^2\rho I^{2j-1}c_s} S. \quad (2)$$

² If σ_r is in μm , I in μA and B in T, the fitting constants c_2 and j have found to be 22.6 and 0.33, respectively. Details are given in [16].

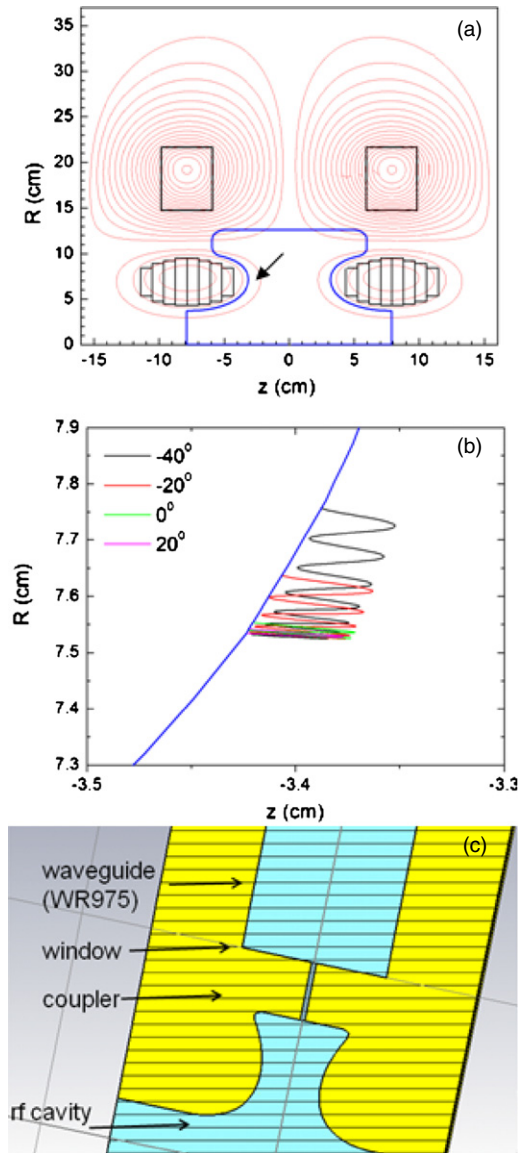


Figure 4. (a) Layout of our proposed magnetically insulated rf cavity and, (b) trajectories of field-emitted electrons at different rf phases from the highest surface field location (the printed arrow) within the cavity shown in (a); and (c) configuration of the experiment to demonstrate magnetic insulation showing the cavity to be coupled radially to the input waveguide.

Assuming that the majority of the electron’s impact energy, E_e , is deposited uniformly within a thermal diffusion length, δ [12], then $E_e = S\delta$, and from equation (2) we obtain

$$E_e = \frac{\delta q \pi c_2^2 \rho I^{2j-1} c_s}{B^2 \tau} \Delta T. \quad (3)$$

From this expression, we can now estimate a ‘safe’ energy, $E_{e,s}$, to avoid damage within the 805 MHz cavity. In our simple model, we assessed $E_{e,s}$ using the following parameters:

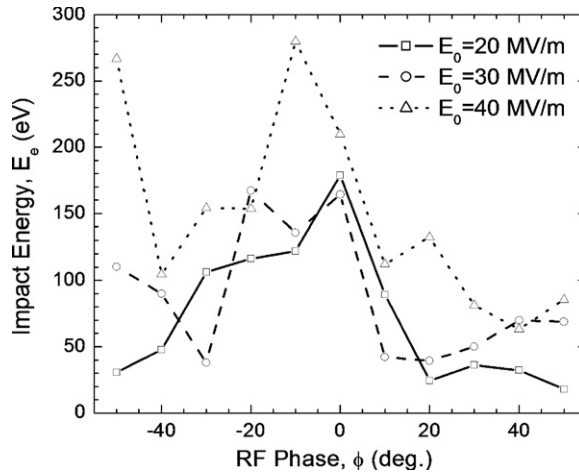


Figure 5. Energies on impact of the returning electrons in figure 4(b) as a function of their initial phase. The axial electric field varies from 20 to 40 MV m⁻¹.

$c_s = 0.385 \text{ J g}^{-1} \text{ }^\circ\text{C}^{-1}$, $\rho = 8.96 \text{ g cm}^{-3}$ (we assume a Cu cavity) and $B \approx 3 \text{ T}$; for the current, we used the value measured in [8], i.e. $I = 0.1 \text{ mA}$, and for ΔT we used $110 \text{ }^\circ\text{C}$ [16] i.e. the temperature required to induce the surface damage from cyclical ohmic heating [14, 15]. Under the assumptions specified above if $E_e < 40 \text{ keV}$, the operation of the cavity is likely to be safe. We point out that even though our calculation was an approximate one, the impact energies are at least an order of magnitude higher and lower, respectively, from this limit in the pillbox cavity and the magnetically insulated cavity. Consequently, we might well expect that the damage created by field emissions must be suppressed significantly in the latter cavity.

Next, we explore the cavity's tolerances to misalignment errors by deliberately displacing the coils. In figure 6(a), we move the coils horizontally up to 5 mm; in figure 6(b) we move the coils the same distance, but vertically. In all cases, both the cavity's position and the accelerating gradient remain fixed. A close examination of figure 6 reveals that the cavity appears more sensitive to positional errors of the vertical coils. This fact may be anticipated simply because the contour of the field lines along the emitter's vicinity in figure 4 change more abruptly in the vertical direction rather than the horizontal. Most importantly, 1–2 mm coil misalignments in both directions do not increase substantially the electron impact energy; thus, operating the cavity under those conditions is likely to be safe.

Before concluding let us make a few more comments about the practical aspects of our proposed magnetically insulated cavity. A simple power estimate can be made by using the relation $P = \frac{(E_0)^2 L}{Z}$, where L is the axial distance of the cavity, Z is shunt impedance per unit length and E_0 is the average axial electric field. By using the parameters from table 1 we find that an average gradient of 25 MV m^{-1} would require 4.7 MW with Q 's of 17700. While it is not yet certain what precise gradients should be used for a muon collider, it becomes evident that magnetically insulated cavities are more demanding in power than pillboxes. A proof-of-principle experiment [25] is underway to provide crucial information on the practical aspects of the concept i.e. power requirements, cavity performance and its tolerances to coil positional errors. In this experiment, the rf power will be generated by a FNAL 12 MW peak-power klystron [20]. The power from the klystron will be delivered through a standard WR 975 waveguide to the cavity by a slot at its outer radius. A high power handling rf

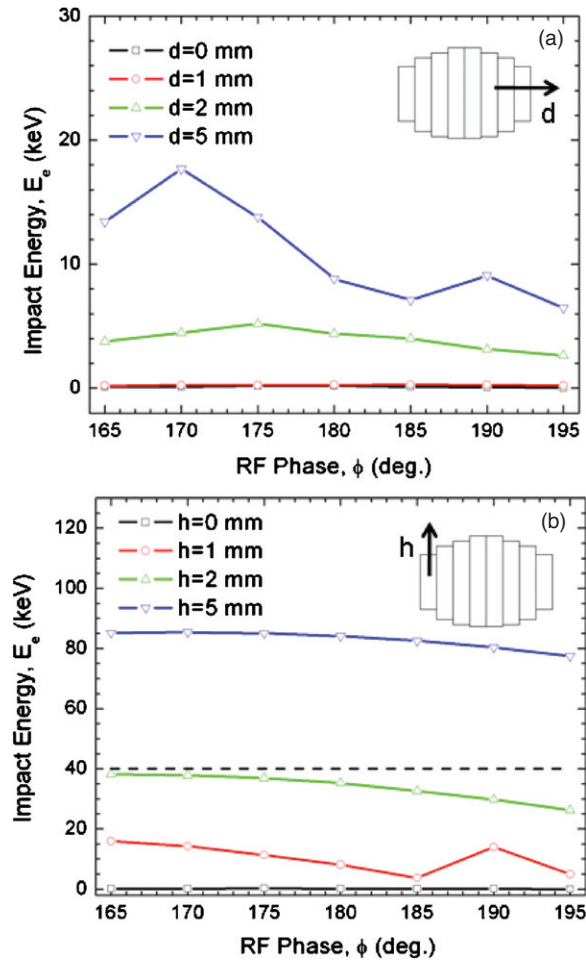


Figure 6. Energies on impact of the returning electrons as a function of their initial phase for different coil displacements. (a) Coils are displaced horizontally by d mm. (b) Coils are displaced vertically by h mm. The axial electric field is $E_0 = 20 \text{ MV m}^{-1}$.

window of a high purity alumina ceramic disc will separate the cavity's vacuum from the air. A preliminary simulation of this configuration with the CST Microwave Studio program³ showed no difficulties and is illustrated in figure 4(c).

4. Demonstration of ionization cooling with magnetically insulated rf

Our main objective in this section is to demonstrate a cooling channel with magnetically insulated cavities and compare its performance to a conventional lattice with pillbox cavities. We consider only transverse cooling, and thus assume a linear transport channel.

As we pointed out in the introduction, because of the way muons are produced, they inherently begin life in a beam with a very large phase-space volume. Ionization cooling is

³ A preliminary simulation with CST Microwave Studio Suite, 2006 was made by J T Keane. The code is available at: <http://www.cst.com>.

Table 2. Comparison of lattice properties between lattices with MI- and PB-cavities.

	PB lattice	MI lattice
Lattice period (cm)	80	80
RF frequency (MHz)	805	805
Peak rf gradient (MV m ⁻¹)	25	25
RF phase from 0-crossing (deg.)	30	30
Maximum axial magnetic field (T)	11.7	13.0
Average momentum (MeV/c)	0.199	0.199
Minimum transverse beta (cm)	4.8	4.7
Axial absorber length (cm)	8.0	10.0
Absorber material	LiH	LiH

therefore necessary to transport the beam through a reasonable accelerator lattice. Typically, each cooling cell must have three components: an rf cavity, an absorber and a solenoid magnet to focus the passing beam and thus eliminate scattering in the absorber. Absorbers with a high rate of energy loss are typically preferred, such as liquid hydrogen or lithium hydride (LiH). Even though cooling can take place at any momentum, it is better if it occurs at the momentum where the curve of the energy loss reaches its minimum so around 200 MeV/c [26].

Having described the basic configuration of a muon cooling lattice, it is important that we emphasize several details for achieving successful cooling. First, in order to eliminate scattering, the minimum value of the transverse beta function β_T should be small over an axial region longer than the absorber. Second, the momentum acceptance of the lattice should overlap the reference momentum, and be larger than the momentum spread of the desired beam. Third, since the solenoid system will introduce angular momentum, altering polarity coils are preferred where the field reverses in alternate cells. We note that a more detailed description about the lattice design can be found in [7].

Figure 7(a) shows the design of a conventional lattice that has been studied [2] for use in the final 6D cooling state for a muon collider. The channel consists of a sequence of identical 80 cm cells, each containing three 8.1 cm long 805 MHz pillbox cavities identical to that shown in figure 1, with 1.9 cm spacing and two 4 cm thick LiH absorbers to assure the energy loss. Moreover, each cell contains two solenoid coils of alternating sign, yielding an approximate sinusoidal variation of the magnetic field in the channel with a peak value of ~ 11.7 T, providing transverse focusing with a low beta value of 4.8 cm. This low value of beta is required as the normalized rms emittance must be reduced < 0.4 mm when the beam exits the channel [2]. The axial length of the solenoids is 19 cm, with an inner radius of 8.1 cm, an outer radius of 13 cm and a current density of 320 A mm^{-2} . Table 2 summarizes the main parameters of this lattice. A problem arises from the fact that, for successful beam transport, the cavities have to maintain a 25 MV m^{-1} gradient within a 5 T magnetic field.

Figure 7(b) illustrates our proposed alternative option for the same cooling lattice but with magnetically insulated cavities (MI lattice). Each cell contains now three 805 MHz magnetically insulated cavities, the geometry of each being identical to that shown in figure 4. The two full and two half elliptical coils on the cavity irises ensure that the magnetic field lines coincide with the cavity's surface. As also mentioned in section 3, we incorporated the outer bucking coils to shape the field lines so that the form of the resulting cavity becomes more efficient in terms of engineering designs. The two orthogonal coils at the far left and right side serve as to focus the beam through the absorber. Table 3 shows the exact position of all coils

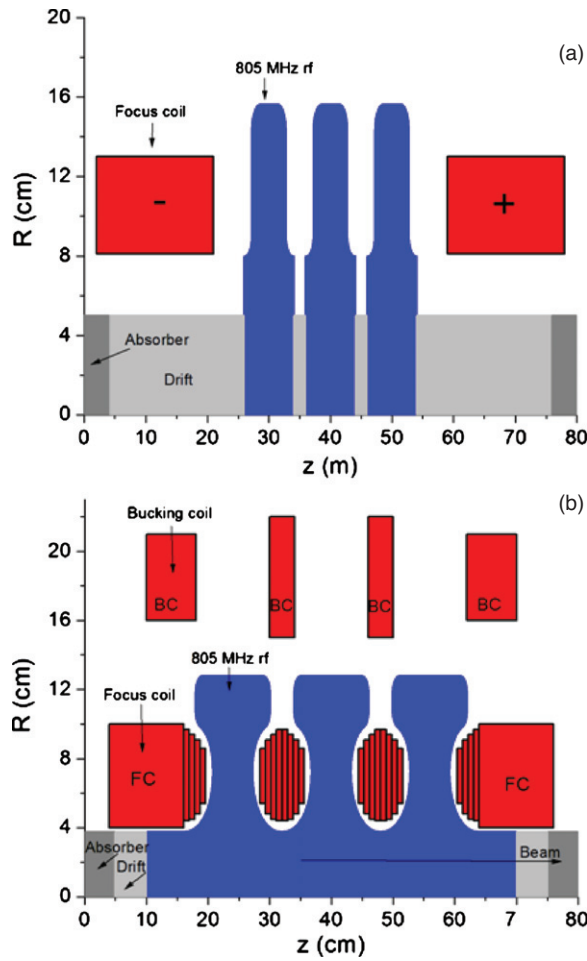


Figure 7. Two alternate cooling scenarios for the final 6D cooling stage of a muon collider: (a) conventional lattice with pillbox cavities; (b) our proposed lattice with magnetically insulated cavities.

as well as their corresponding current densities. Table 2 summarizes the main parameters of the MI lattice and compares them to the parameters of the aforementioned pillbox (PB) lattice.

For our particle tracking simulations, we used ICOOL [27], a tracking code developed at Brookhaven National Laboratory that is widely used in simulations for the neutrino factory and muon colliders. The code covers all relevant physical processes (e.g. energy loss, straggling and multiple scattering) and incorporates electromagnetic fields that satisfy Maxwell’s equations. To compare consistently the performance of our proposed MI lattice with a conventional PB lattice, we assumed that both configurations are driven by an equivalent in rms sense muon beam (same rms size and emittance).

In figure 8 we examine the physical parameters of the MI lattice and PB lattice. For our initial studies, we consider a linear channel with the magnetic field present, but no rf cavities or absorbers. Note that the solid circles and open squares correspond to the MI- and PB lattice, respectively. Figure 8(a) plots the transverse beta as a function of the muon momentum at

Table 3. Characteristics of a magnetically insulated cooling cell. Note that z and dz are the axial position and axial length of the coils, respectively. Also R and dR are the inner radius and radial extend of the coils, respectively.

z (cm)	dz (cm)	R (cm)	dR (cm)	J (A mm ⁻²)
4	12.0	4.0	6.0	-300.0
10	8.0	16.0	5.0	318.6
16	0.9	4.4	5.3	-324.0
16.9	0.9	4.5	4.9	-324.0
17.8	0.9	4.8	4.3	-324.0
18.7	0.9	5.4	3.2	-324.0
28.4	0.9	5.4	3.2	324.0
29.3	0.9	4.8	4.3	324.0
30.0	4.0	15.0	7.0	-362.6
30.2	0.9	4.5	4.9	324.0
31.1	0.9	4.4	5.3	324.0
32	0.9	4.4	5.3	324.0
32.9	0.9	4.5	4.9	324.0
33.8	0.9	4.8	4.3	324.0
34.7	0.9	5.4	3.2	324.0
44.4	0.9	5.4	3.2	-324.0
45.3	0.9	4.8	4.3	-324.0
46	4.0	15.0	7.0	362.6
46.2	0.9	4.5	4.9	-324.0
47.1	0.9	4.4	5.3	-324.0
48	0.9	4.4	5.3	-324.0
48.9	0.9	4.5	4.9	-324.0
49.8	0.9	4.8	4.3	-324.0
50.7	0.9	5.4	3.2	-324.0
60.4	0.9	5.4	3.2	324.0
61.3	0.9	4.8	4.3	324.0
62	8.0	16.0	5.0	-318.6
62.2	0.9	4.5	4.9	324.0
63.1	0.9	4.4	5.3	324.0
64.0	12.0	4.0	6.0	300.0

the center of the absorber ($z = 0$). It demonstrates that the MI lattice transmits particles in the momentum band 165–233 MeV/ c with a central momentum of 199 MeV/ c . Figure 8(b) illustrates the beta function at the central momentum as a function of the axial position in the cell. Figure 8(c) depicts the longitudinal magnetic field along the cell axis. These figures highlight the following points: first, the MI lattice, like the PB lattice, has the same momentum acceptance with the desired central (reference) momentum ≈ 200 MeV/ c . Second, the beta in both cases remains minimal for ≈ 4 cm, matching well with the absorber's axial length. Moreover, in both lattices, the minimum value of β at the center of the absorber at central momentum was ~ 4.7 cm, implying that they can cool up to the same equilibrium emittance. Third, in order to achieve the desired β the MI lattice requires a stronger magnetic-peak magnetic field (i.e. $B_0 = 13.0$ T), and has richer longitudinal harmonics of the axial fields; these harmonics initially were thought to entail considerable particle loss.

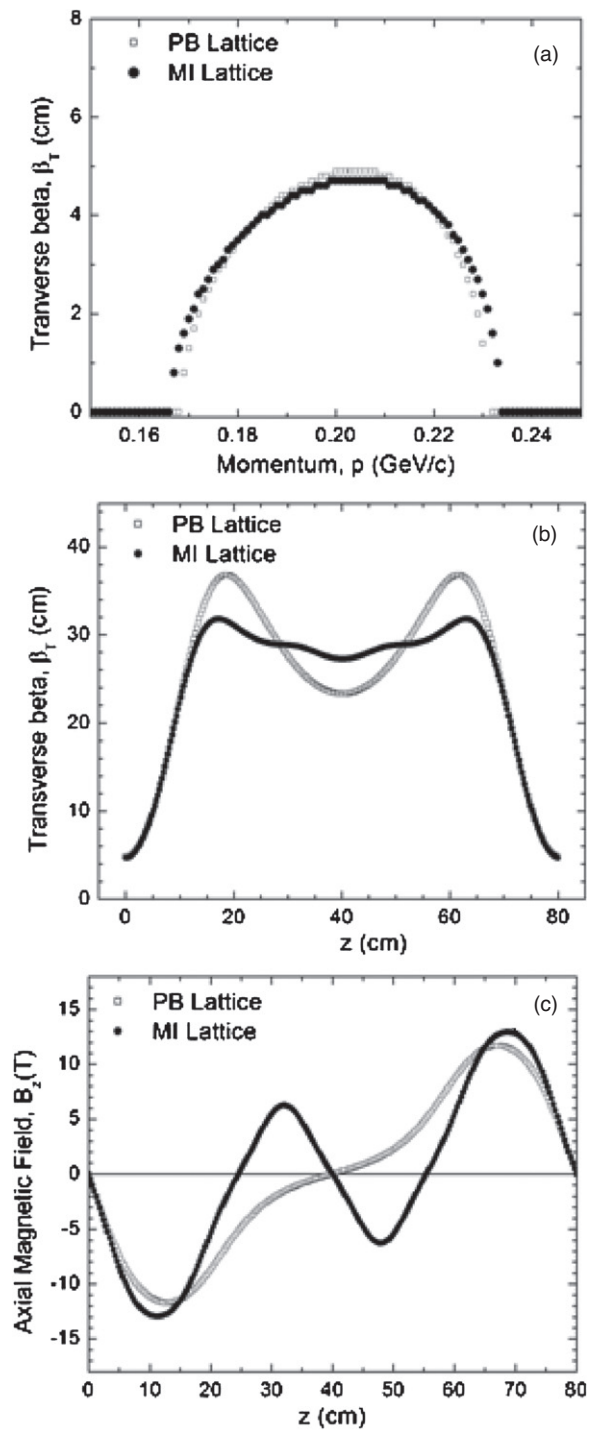


Figure 8. (a) Beta function versus muon momentum at the center of the absorber ($z = 0$); (b) beta function at central momentum versus position in the cell and (c) axial magnetic field versus position in the cell. Note that the open squares correspond to the PB lattice, and the filled circles correspond to the MI lattice.

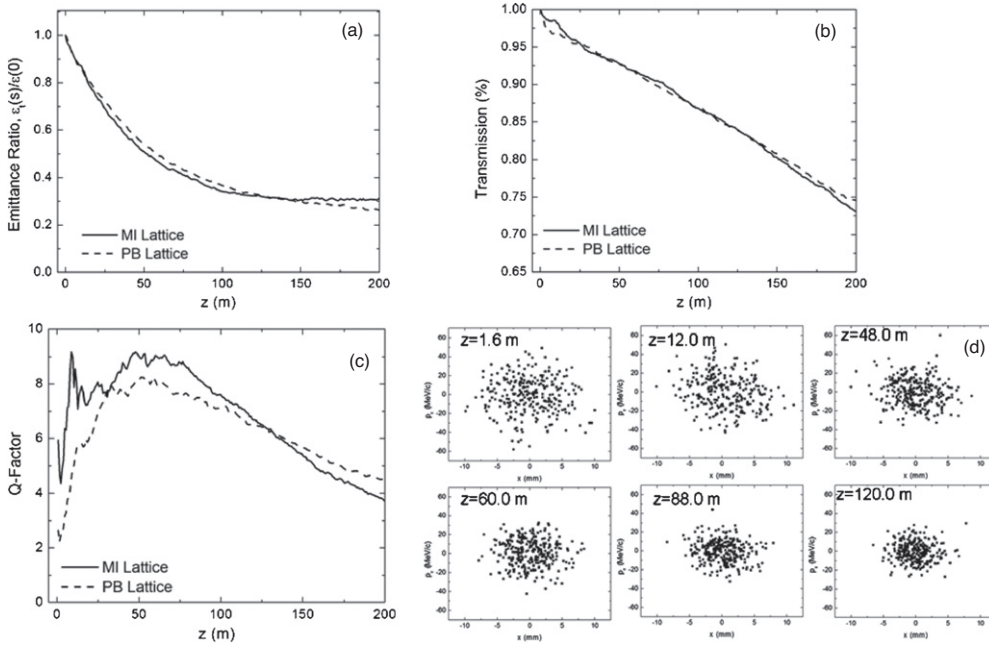


Figure 9. Cooling performance of our proposed magnetically insulated channel: (a) transverse normalized emittance versus distance; (b) transmission of muons versus distance; (c) merit factor, Q versus distance and (d) reduction of the transverse muon phase space due to cooling.

Quantitatively, three factors determine the performance of a cooling channel. First is the lattice transmission T , a factor that quantifies the number of particles passing through the lattice. Second is the ratio $\varepsilon_t(z)/\varepsilon_t(0)$, wherein $\varepsilon_t(z)$ is the transverse emittance at any point z , and $\varepsilon_t(0)$ is the starting emittance. Third is the Q factor [7], a merit factor commonly used in evaluating the lattice’s cooling performance, and is defined as the ratio of the relative change of emittance to the relative change of the particle flux. Quantitatively, an effective average Q is defined by $Q_{\text{eff}} = \frac{\text{Ln}\left(\frac{\varepsilon_t(z)}{\varepsilon_t(0)}\right)}{\text{Ln}\left(\frac{N(z)}{N(0)}\right)}$, where $N(z)$ is the total number of muons surviving at position z . As a baseline in our simulation we chose the ones reported in [28] as representative target values for the final 6D cooling of a muon collider: $T = 0.72$, $\varepsilon_t(z)/\varepsilon_t(0) = 3$ and $Q_{\text{eff}} = 8$.

Figure 9 illustrates the cooling performance of our magnetically insulated lattice (black line). These results have been obtained by post-processing the output of ICOOL using ECALC9,⁴ an emittance calculation program customarily employed for the Muon collaboration. Figure 9(a) displays the ratio of the transverse emittance along the lattice to its initial value at $z = 0$. In comparison to the PB lattice, the initial cooling rate of the MI lattice is larger, most likely due its 2 cm longer absorber. After about 130 m, emittance has fallen by a factor of 3.5, with a transmission of 70% (see Figure 9(b)). There is no further cooling beyond that point. The Q factor, Q_{eff} , remains close to 8 (see figure 9(c)). Interestingly, the MI lattice performs similarly to the PB lattice (dashed line) with transmission, Q factor and the cooling factor that all meet the aforementioned specified requirements. Those facts

⁴ ECALC 9 is a Fortran code written by G Penn, University of California, Berkeley.

suggest that our scheme of a cooling channel with magnetically insulated cavities is likely a viable choice for a muon collider and/or a neutrino factory.

Figure 9(d) illustrates the cooling effect in the transverse direction, where we show the transverse trace space at different locations along the lattice. The reduction of the phase space is clearly visible as the beam propagates through the lattice. So far, we assumed a linear transport channel. We note that demonstrating 6D cooling is a more complex problem as it requires a bend magnet to introduce dispersion [29] so that 6D cooling results from emittance exchange between the transverse- and longitudinal directions. This important subject is beyond the scope of this work but will be addressed in a future work.

5. Summary

RF breakdown in magnetic fields is a continuing problem that limits the performance of muon accelerators. It is believed that the cause of breakdown is the damage induced by the impact with the cavity's surface of a focused beam of field-emitted electrons. In this paper, we presented a novel design of a magnetically insulated cavity wherein the magnetic fields are parallel to its emitting surfaces. We showed that, with magnetic insulation, the field-emitted electrons impact the cavity surface with energies three orders of magnitude less than in conventional pillbox cavities; consequently, damage from field emission is suppressed significantly. We presented a conceptual design of a cooling lattice with magnetically insulated cavities and examined its performance. Similar to a conventional pillbox cavity lattice, it successfully transported and cooled the muon beam.

Theoretically, it will be interesting to pursue additional simulations to detail the effects from secondary emissions, or from the emitter's shape and dimensions. Experimentally, there is a clear need for designed tests to study, systematically, the performance of magnetically insulated cavities. There are some engineering challenges to be studied as well; for instance, the selection of the material for the coils, the calculation of the forces between the coils and the space needed between the coils and cavity wall.

We conclude that the viability of the currently used PB lattice for a muon collider or a neutrino factory largely depends on whether the rf cavities work in a magnetic field. It remains to be proved experimentally that the rf pillbox cavities at 16–25 MV m⁻¹ do not breakdown in magnetic fields up to 5–6 T and so far this is not the case. Lacking these data, there is a strong argument for considering, as an alternative, our magnetically insulated cooling channel that shields the cavity from those strong magnetic fields. We demonstrated in this study that such a lattice is indeed a feasible option for a muon accelerator as it performs equally well to a conventional lattice with pillbox cavities.

Acknowledgments

The authors are grateful to J S Berg, R C Fernow, H Kirk, J Kolonko, D Cline, B Weggel, J T Keane and J Norem for their useful discussions. The authors also wish to thank A Woodhead for reading the paper and making useful suggestions. This work is supported by the US Department of Energy, contract no DE-AC02-98CH10886.

References

- [1] Apollonio M *et al* 2009 *JINST* **4** P07001
- [2] Palmer R B 2009 *Proc. 2009 Particle Accelerator Conf. TUIGRI03, 2009*
- [3] Johnstone C, Berz M and Makino K 2006 *Nucl. Instrum. Methods A* **558** 282

- [4] Skrinsky A N and Parkhomchuk V V 1981 *Sov. J. Part. Nucl.* **12** 223
- [5] Neuffer D 2004 *Nucl. Instrum. Methods Phys. Res. A* **532** 26
- [6] Ankenbrandt C, Bogacz S A, Bross A, Geer S, Johnstone C, Neuffer D and Popovic M 2009 *Phys. Rev. ST Accel. Beams* **12** 070101
- [7] Palmer R B *et al* 2005 *Phys. Rev. ST Accel. Beams* **8** 061003
- [8] Norem J, Wu V, Moretti A, Popovic M, Qian Z, Torun Y and Solomey N 2003 *Phys. Rev. ST Accel. Beams* **6** 072001
- [9] Bross A 2009 Summary of 201 MHz running, NFMCC Friday Meeting, <http://www.fnal.gov/projects/muon collider/FridayMeetings/>
- [10] Moretti A, Qian Z, Norem J, Torun Y, Li D and Zisman M 2005 *Phys. Rev. ST Accel. Beams* **10** 072001
- [11] Rimmer R A 2009 private communication
- [12] Palmer R B, Fernow R C, Gallardo J C, Stratakis D and Li D 2009 *Phys. Rev. ST Accel. Beams* **12** 031002
- [13] Jensen K L, Lau Y Y, Feldman D W and O'Shea P G 2008 *Phys. Rev. ST Accel. Beams* **11** 081001
- [14] Tantawi S G *et al* 2007 *Proc. of PAC07, Albuquerque (NM, USA)* p 2370
- [15] Pritzkau D P and Siemann R H 2002 *Phys. Rev. ST Accel. Beams* **5** 112002
- [16] Stratakis D, Gallardo J C and Palmer R B 2010 *Nucl. Instrum. Methods A* **620** 147
- [17] Winterberg F 1973 *Nature* **246** 299
- [18] Grisham L R 2009 *Phys. Plasmas* **16** 043111
- [19] Novak B M, Smith I R and Brown J 2002 *J. Phys. D: Appl. Phys.* **35** 1467
- [20] Li D *et al* 2003 *J. Phys. G: Nucl. Part. Phys.* **29** 1683
- [21] Fernow R C 2009 NFMCC *Technical Note 533* <http://nfmcc-docdb.fnal.gov/cgi-bin/DocumentDatabase/>
- [22] Billen J H and Young L 1993 *Proc. 1993 Particle Accelerator Conf.* p 790
- [23] Fowler R and Nordheim L 1928 *Proc. R. Soc. A* **119** 173
- [24] Ge L *et al* 2009 *Proc. 2009 Particle Accelerator Conf. (Vancouver, Canada) WE5PFP020*
- [25] Keane J T *MuCool RF III Workshop, 'Design of a Demonstration of Magnetic Insulation'* <http://mice.iit.edu/mta/mcrf3/>
- [26] Fernow R C and Palmer R B 2006 *Phys. Rev. ST Accel. Beams* **10** 064001
- [27] Fernow R C 1999 *Proc. 1999 Particle Accelerator Conf., New York (IEEE, New York, 1999)* p 3020
- [28] Palmer R B 2009 *Muon Collider Design Workshop (Newport News, VA)* <http://conferences.jlab.org/muon/talks/Palmer.pdf>.
- [29] Snopok P, Hanson G and Kleir A 2009 *Int. J. Mod. Phys. A* **24** 987